World Applied Sciences Journal 10 (3): 342-347, 2010
ISSN 1818-4952

Improving Gain and Saturation Output Power in Single-Quantum-Well Semiconductor Optical Amplifiers by Injection Current

[1]*Maryam Babaei,* [2]*Seyedeh Somayeh Hosseini and* [3]*Satar Mirza Kuchaki*

[1]Islamic Azad University, Khoramabad Branch, Iran
[2]Islamic Azad University, Gonbad Kavoos Branch, Iran
[3]Iran University of Science and Technology, School of Electronic Engineering, Tehran, Iran

Abstract: The gain and saturation output power of In $_x$Ga$_{1-x}$ As-GaAs single quantum-well semiconductor optical amplifiers is calculated. A single quantum-well semiconductor optical amplifiers will have a positive gain versus I_{inj}=0.37I_{th}. The gain and saturation output power increases with the I_{inj} /I_{th} enhancement.

Key words: Gain · Saturation output power · Semiconductor optical amplifier · Rate equation · Injection current

INTRODUCTION

Semiconductor optical amplifiers (SOAs) are optoelectronic devices witch offer very promising features for the optical treatment of information. They offer the distinct asset of performing multiple operations at the same time and the user can take advantage of both the linear and nonlinear behavior of SOA' s. SOAs are currently realized in a variety of different structures, with the active region consisting of bulk materials [1] or quantum wells (QWs) [2]. QW have successfully been used in laser to give low threshold currents, high-speed operation and narrow line widths [3], [4]. These advantages arise from to basic properties 0f the QW's in the laser: the small active volume in which you need to achieve population inversion and the high differential gain [5]. The use of quantum wells for optical amplifiers has surprisingly received much less attention [5].

An ideal SOA should possess a large gain of frequency bandwidth and a high saturation power. In linear and nonlinear applications, SOAs with high bit rates have received remarkable attention; this highlights the importance of gain recovery rate enhancement. In conventional SOAs this rate, which is limited to carrier recovery rate and related to input power and injection current. Optical amplification usually reduces population inversion. As the input power increases, electrons' reduction rate increases to such an extent that the population inversion cannot remain fixed; this results in a reduction in gain [6, 7]. Gain saturation, which is one of the most important factors in optical amplification process, is determined in light of saturation output power and causes inconvenience in the shape of the amplified signal. Saturation output power impacts the dynamic range and restricts the maximum accessible amplifying power [8].

In this paper we calculated quantum-well gain as a function of current density in the standard way [5] and extend the calculation to consider the gain and saturation output power of InGaAs-GaAs laser Amplifier and we offers a solution to above problem by enhancing gain and saturation output power by means of injection current enhancement.

The method used here the Finite Difference Method (FDM) [9]. The Schrodinger equation is solved numerically first to determine the energy states within a quantum well and then by injection current, the Pseudo-Fermi levels are calculated. The gain is then calculated based on the Fermi's golden role. This in turn yields threshold current density. In order to model the behavior of the amplifier, the change carrier and the photon rate equation are solved in coupled from through finite difference method and self consistency [10, 11].

THEORY

The Rate Equation Model: Fig. 1 illustrates the modeled transport processes in a SQW semiconductor lasers and Amplifiers [12]. The simulated amplifiers have a structure defined as follows: In$_2$Ga$_8$ As-GaAs. Generally,

Corresponding Author: S.S. Hosseini, Islamic Azad University, Gonbad Kavoos Branch, Iran.
E-mail: somayeh.hosseinix@yahoo.com.

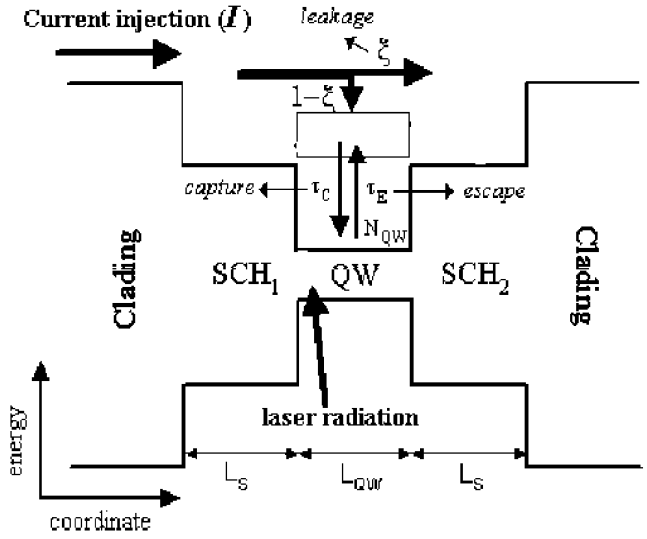

Fig. 1: Carrier transport processes being modeled in SQW amplifier structures

in this simulation the wavelength of the input signal is constant and the maximum gain of the amplifier is at a wavelength of 1.55μm.

Two independent carrier rate-equations are used for the separate confinement heterostructure (SCH) layer [13]: one for the region to the left of the well (N_{sch1}) and another for the on to the right (N_{sch2}). They are normalized with respect to the volume 0f each SCH region [13, 14].

The 2D carrier (N_1) distribution in the well is modeled by a third equation. This 2-D carrier is normalized with respect to the volume of the equation well [13, 14]. If we assume injection from left of the SCH, then the rate of change in the carrier density in the left SCH region is.

$$\frac{dN_{sch1}}{dt}=\frac{\eta_i I}{qV_{sch}}-\frac{N_{sch1}}{\tau_s}-\frac{N_{sch1}}{\tau_{nsch}(N_{sch1})}+\frac{N_1}{\tau_e}.(\frac{V_{well}}{V_{sch}})+\xi\frac{N_{sch2}}{\tau_s} \quad (1)$$

The rate of change in 2-D carrier density in the quantum well is:

$$\frac{dN_1}{dt}=(1-\xi)\frac{N_{sch1}}{\tau_s}\cdot\left(\frac{V_{sch}}{V_{well}}\right)+(1-\xi)\frac{N_{sch1}}{\tau_s}\cdot\left(\frac{V_{sch}}{V_{well}}\right)$$
$$-\frac{2N_1}{\tau_e}-\frac{N_1}{\tau_n(N_1)}-\Gamma_w v_g g(N_1)(1-\varepsilon\Gamma_w S)S \quad (2)$$

For the SCH region to the right, the rate of change in the carrier density is:

$$\frac{dN_{sch2}}{dt}=-\frac{N_{sch2}}{\tau_s}-\frac{N_{sch2}}{\tau_{nsch}(N_{sch2})}+\frac{N_1}{\tau_e}.(\frac{V_{well}}{V_{sch}})+\xi\frac{N_{sch1}}{\tau_s} \quad (3)$$

The r ate of change in the photon density is given by the usual equation:

$$\frac{dS}{dt}=\Gamma_w v_g g(N_1)(1-\varepsilon\Gamma_w S)S-\frac{S}{\tau_p}+\beta\frac{N_1}{\tau_n(N_1)} \quad (4)$$

Where I is the injection current, q is the electronic change, Such is the volume of one side of the SCH layer, τ_s is the carrier transport time in the SCH region, τ_e is the carrier thermion emission/escape time, ξ is the leakage factor mentioned earlier, Γ_W is the optical confinement factor of the single quantum well, g(N) is the carrier-density dependent gain, S is the photon density normalized with respect to the volume of the quantum well, Vwell, τ_p is the photon life time, ε is the gain compression factor, β is the spontaneous emission factor, η_i is the internal quantum efficiency, v_g is the group velocity and both τ_{nsch} and τ_n are the carrier recombination life time in the SCH region and in the quantum well, respectively [12]. The carrier-density dependent carrier recombination lifetime are given by

$$\tau_n=[A+BN+CN^2]^{-1}$$

Where A, B and C are the usual recombination coefficients. The set of values for coefficients A, B and C shown in Table 1 requires some clarification.

Table 1: Parameters Of the Rate-equation Model [12-14], [18, 21, 22].

Symbol	Parameter	Value
Inj. eff	η_i	0.95
Width (SCH)	L_{SCH}	130 nm
Width (QW)	L_W	4.8 nm
Therm. Em.	τ_e	20 ps
Transport time	τs	13 ps
Gain comp. factor	ε	$1.0*10^{-17}$ cm^3
Internal loss	α_{int}	11.8 cm^{-1}
Temperature	T	300 K
Optical conf.	Γ_W	0.02
Initial dens. (SCH)	N_{sch}	$4*10^{11}$ cm^{-3}
Initial dens. (QW)	N_0	$4*10^{11}$ cm^{-3}
Threshold dens.	N_{th}	$9*10^{17}$ cm^{-3}
Traps coeff.	A	$1.1*10^{8}$ s^{-1}
Spont. Coeff.	B	$0.7*10^{-10}$ cm^{3}s^{-1}
Auger coeff.	C	$0.6*10^{-29}$ cm^{6}s^{-1}
Leakage factor	ξ	0
Spont. Em. factor	β	$1*10^{-4}$
Material gain coeff.	G_0	1500 cm^{-1}
Group vel.	v_g	$8.5*10^7$ m/s

By definition τ_e used here is twice that used by Nagarajan *et al.* [13-15]. Also $(1-\varepsilon\Gamma_W S)$ is used because the photon density is defined assuming all the photons travel within the active region [16, 12].

Gain: The carrier-density dependent gain of a single quantum well is taken as the logarithmic gain-current density relationship as defined in [17]:

$$g(N) = G_0 \ln(\frac{AN + BN^2 + CN^3}{AN_0 + BN_0^2 + CN_0^3}) \quad (5)$$

Where N is the carrier density in that particular quantum well, G_0 is the gain coefficient and $AN+BN^2+CN^3$ accounts explicity for the role of each recombination process through the recombination coefficients A for Capture at trap centers, B for spontaneous emission and C for Auger recombination [18]. The benefits of incorporating strain in QW devices should be reflected in an increase in the value of G_0 [19] and a reduction in both the transparency current density [19, 20] and Auger recombination rate [20]. The usual linear form of the gain is only suitable for small signal analysis, [12-14].

Broad-Area Threshold Current-Density of SQW Amplifiers: The Broad-Area Threshold current densities 0f 980nm InGaAs-GaAs SQW laser have been studied analytically by Coleman *et al.* [21]. The equation for the threshold current density of SQW laser is:

$$J_{th} = \frac{J_0}{\eta_i} \exp[\frac{\alpha_{int} + \alpha_m}{\Gamma_w G_0}] \quad (6)$$

Where α_{int} is internal loss, α_m is the mirror loss and both J_{th} and J_0 are the current densities at threshold and transparency, respectively. These current densities can be expressed in terms of the corresponding carrier densities at threshold, N_{th} and transparency, N_0 and the width of the quantum well, Lz [12, 17].

$$J_0 = qL_Z(AN_0 + BN_0^2 + CN_0^3) \quad (7)$$

$$J_{th} = \frac{qL_Z}{\eta_i}\left(AN_{th} + BN_{th}^2 + CN_{th}^3\right) \quad (8)$$

SIMULATIN RESULTS

The results of the analysis of quantum-structure amplifiers show that the injection current of the traveling-wave semiconductor amplifier falls below the threshold current. Also, in the amplifiers of the traveling-wave type the resistance of both ends is set to zero in the ideal condition although in reality they put up small quantities of resistance. All the parameters employed for the simulation are presented in Table 1.

Initially, we will show how much injection current is required for an amplifier to result in gain. Certainly, the larger the input power is (before reaching the saturation level), the better the amplifying conditions are provided in smaller currents. Here the input amplifier is assumed equal to -60 dBm. As plotted in Fig. 2 the amplifier will have a larger gain versus I_{inj} /I_{th}. It is worth noting that the larger the current used for the amplifier injection, the smaller the currents at which the amplifier will be saturated.

In order to calculate the input power, the amplifier's behavior in different time-intervals should be understood. The time-intervals should be specified in a way that makes it possible to measure the precise input power which begins in each particular time. Having performed different observations, the range from 65-dBm to -15 dBm was selected as the optimally fitting range. In Fig. 3, I_{inj}/I_{th} is equal to 0.9 and the amplifier is divided into 20 sections. As seen in the figure, the amplifier's gain begins to decline around -52 dbm, which happens under the influence of saturation output power.

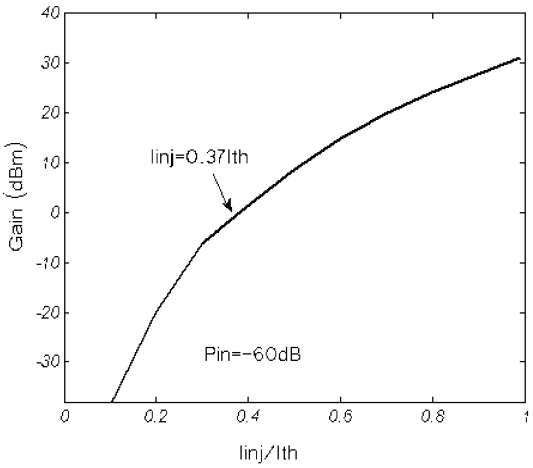

Fig. 2: Amplifier's gain versus injection current

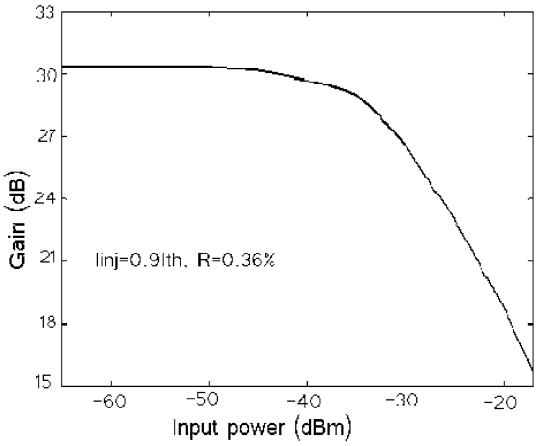

Fig. 3: Amplifier's gain versus input power at I_{inj} / Ith=0.9

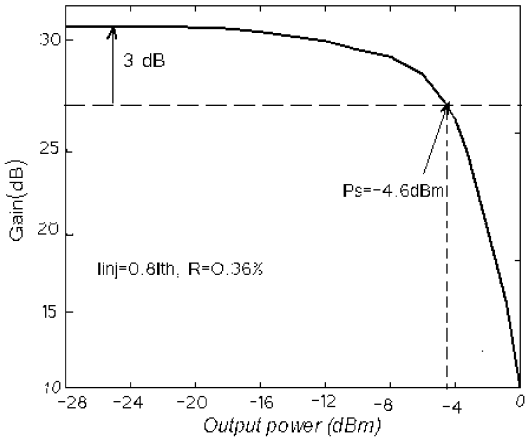

Fig. 4: Amplifier's gain versus input power at I_{inj}/I_{th}=0.9

As the input power increases, the amplifier cannot sufficiently amplify the input signal; this is because the constant population inversion caused by a constant injection current is negated by the input signal and hence

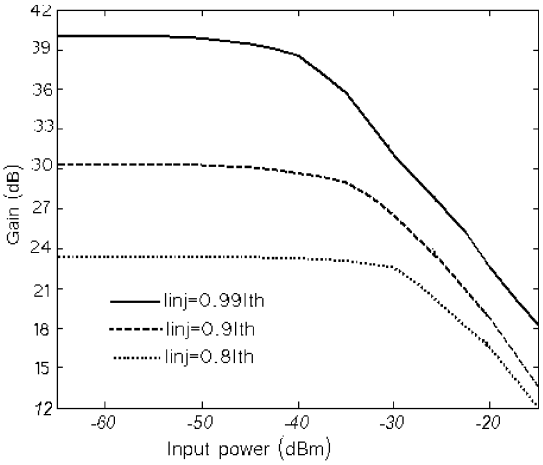

Fig. 5: Amplifier gain versus input power at different injection currents

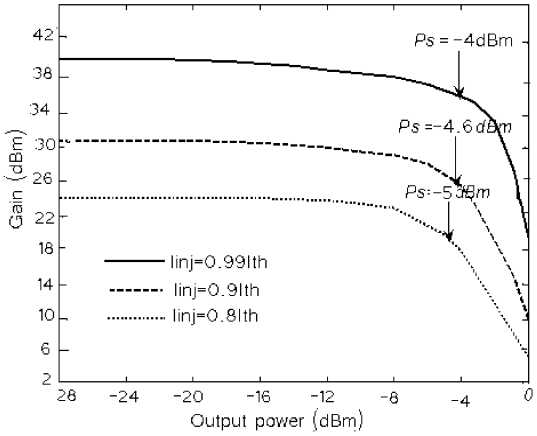

Fig. 6: Amplifier's gain versus input power at different injection currents

begins to decline; this results in the reduction of the amplifier's gain, which is directly related to carrier density.

In order to measure the saturation output power, gain changes should be plotted as a function of output power. In so doing, the range needs to be relocated since in the powers larger than the output power, the amplifier will become saturated. In Fig. 4 the curve has been plotted at I_{inj} / I_{th}= 0.9 with Psat=4.6 dBm.

In Fig. 5 the impacts of the injection current changes on the amplifier's behavior is plotted. Not surprisingly, as the current increases the amplifier's gain grows larger than its previous magnitude. This figure is plotted at three quantities, I_{inj}/I_{th} =0.8, 0.9 and 0.99.

The total sum of the injection carrier density increases with the injection current improvement. The closer the amplifier injection current to the threshold level, the smaller the powers at which the amplifier becomes saturated.

Another notable point is the change in the magnitude of the output power. In Fig. 6 the saturation output power increases with the I_{inj} /I_{th} enhancement because in this state the occurred population inversion rate keeps constant as a function of a larger input power. Saturation powers will be -4dBm, -4.6dBm and -5.05respectively.

CONCLUSION

In order to have a higher saturation output power, the current increases along with the injected light. The injected light should have a wavelength around gain peak. The total sum of the injection carrier density increases with the injection current improvement. The closer the amplifier injection current to the threshold level, the smaller the powers at which the amplifier becomes saturated.

Increase in the amplifier injection results in a growth in saturation output power and the increase in the input powers results in further changes in gain and output signal wave, thereby increasing the output signal wave at the input powers larger than saturation.

REFERENCES

1. Doussiere, P., F. Pommereau, J.Y. Emery, R. Ngo, J.L. Lafragette, P. Aubert, L. Goldstein, T. Ducellier, M. Bachmann and G. Laube, 1996. 1550 nm polarization independent DBR gain clamped SOA with high dynamic input power range," in Proc. ECOC'96, Oslo, Norway, pp: 3. 169-3.172.
2. Thijs, P.J.A., L.F. Tiemeijer, J.J.M. Binsma and T. Van Dongen, 1994. Progress in long- wavelenght strained-layer InGaAs(P) quantum-well semiconductor lasers and amplifiers, IEEE J. Quantum Electron., 30: 477-499.
3. Tsang, W.T., 1981. Extremely low threshold (AlGa) As modified multi- quantum well heterostructure lasers grown by molecular beam epitaxy, Appl. Phys. Lett., 39: 786-787.
4. Kobayashi, K. and I. Mito, 1988. Single frequency tunable laser diodes, J. Lightwave Technol., LT-6, pp: 1623-1633.
5. Stevens, P.J. and T. Mukai, 1990. Predicted performance of quantum-well GaAs- (GaAl)As optical amplifiers, IEEE J. Quantum Electron, 26(11): 1910-1917.
6. Yoshino and K. Inoue, 1996. Improvement of saturation output power in a amplifier through pumping light injection, IEEE Photon. Technol. Lett., 8(1): 58-59.
7. Tang, J.M. and K.A. Shore, 1999. Active picosecond optical pulse compression in semiconductor optical amplifiers, IEEE J. Quantum Electron.
8. Verdiel, J.M., M. Ziari and A. Mathur, 0000. Semiconductor optical amplifiers, IEEE Database. WB2.
9. Gerald, C. and P.O. Wheatly, 2002. Applied Numerical Analysis, Adbison-Wesley, 6th Edn.
10. Silver, M., A.F. Phillips, A.R. Adams, P.D. Greene and A.J. Collar, 2000. Design and ASE Characteristics of 1550-nm polarization-insensitive semiconductor optical amplifiers containing tensile and compressive wells, IEEE J. Quantum Electron, 36(1).
11. Lysak, V.V., H. Kawaguchi and I.A. Sukhoivanov, 2005. Gain spectra and saturation power of asymmetrical multiple quantum well well semiconductor optical amplifiers, IEE Proc-Optoeiectron, 152(2).
12. Nguyan, L.V.T., A.J. Lowery, P.C.R. Gurney and D. Novak, 1995. A Time- Domain Model for High-speed Quantum-Well laser Including Carrier Transort Effects, IEEE J. Quantum Electron, 1(2).
13. Nagarajan, R., T. Fukushima, M. Ishikawa, J.E. Bowers, R.S. Geels and L.A. Coldren, 1992. Transport limits in high-speed quantum-well lasers: Experiment and theory," IEEE Photon. Technol. Lett., 4: 121-123.
14. Nagarajan, R., M. Ishikawa, T. Fukushima, R.S. Geels and J.E. Bowers, 1992. High speed quantum-well lasers and carrier transport effects. IEEE J. Quantum Electron, 28: 1990-2008.
15. Nagarajan, R., T. Fukushima, S.W. Corzine and J.E. Bowers, 1991. Effects of carrier transport on high-speed quantum well lasers, Appl. Phys. Lett., 59: 1835-1836.
16. Tessler, N., R. Nagar and G. Eisenstein, 1992. Structure dependent modulation responses in quantum-well lasers, IEEE J. Quantum Electron, 28: 2242-2250.
17. DeTample, T.A. and C.M. Herzinger, 1993. On the semiconductor laser logarithmic gain-current density relation, IEEE J. Quantum Electron, 29: 1246-1252.
18. Reale, A., Aldo Di Carlo, P. Lugli, D. Campi, C. Cacciatore, A. Stano and G. Fornuto, 1999. Study of gain compression mechanisms in multiple-quantum-well $In_{1-x}Ga_x$ As semiconductor optical amplifiers, IEEE J. Quantum Electron., 35: 1697-1703.
19. Lin, C.H. and Y.H. Lo, 1993. Empirical formulas for design and optimization of 1.55μm InGaAs/InGaAsP strained-quantum-well lasers, IEEE Photon. Technol. Lett., 5: 288-290.

20. Zou, Y., J.S. Osinski, P. Grodzinski, P.D. Dapkus, W. Rideout, W.F. Sharfin and F.D. Crawford, 1992. "Experimental verification of strain benefits in 1.5 μm semiconductor lasers by carrier lifetime and gain measurements, IEEE Photon. Technol. Lett., 4: 1315-1318.
21. Coleman, J.J., K.J. Beernink and M.E. Givens, 1992. Threshold current density in strained layer In_xGa_{1-x} As-GaAs quantum-well heterostructure lasers, IEEE J. Quantum Electron., 28: 1983-1989.
22. Tiwari, S. and J.M. Woodall, 1994. Experimental comparison of strained quantum-wire and quantum well laser characteristics, Appl. Phys. Lett., 64: 2211-2213.